A new NRF2 activator for the treatment of human metabolic dysfunction-associated fatty liver disease

Adel Hammoutene[1,2], Samira Laouirem[1], Miguel Albuquerque[1,3], Nathalie Colnot[3], Angélique Brzustowski[1], Dominique Valla[1], Nicolas Provost[2], Philippe Delerive[2], Valérie Paradis[1,3], on behalf of the QUID-NASH research group

Table of contents

QUID-NASH Research Group members

QUID-NASH project coordinators: Prof. Dominique Valla & Angélique Brzustowski

Beaujon hospital group (Université de Paris, Assistance Publique-Hôpitaux de Paris and Inserm CRI-UMR1149): Laurent Castéra, Pierre-Emmanuel Rautou, Bernard Van Beers, Valérie Vilgrain, Philippe Garteiser, Marco Diogardi-Burbio, Sabrina Doblas, Valérie Paradis, Pierre Bedossa, Miguel Albuquerque and Adel Hammoutene

Lariboisière hospital group (Université de Paris, Assistance Publique-Hôpitaux de Paris and Inserm U1138**:** Jean-François Gautier, Tiphaine Vidal-Trécan, Jean-Pierre Riveline, Jean-Baptiste Julla.

Cochin hospital group (Université de Paris, Assistance Publique-Hôpitaux de Paris and Institut Cochin): Christian Boitard, Etienne Larger, Stanislas Pol, Anaïs Vallet-Pichard, Benoît Terris, Béatrice Parfait, Catherine Postic, Agnès Lehuen, Amine Toubal, Camille Rousseau, Blandine Fruchet, Pauline Soulard, Zouriatou Gouda, Michel Vidaud, Franck Letourneur, Gilles Renault, Raphaël Scharfmann

Necker-Enfants Malades hospital group (Université de Paris, Assistance Publique-Hôpitaux de Paris): Jean-Michel Corréas

European hospital George Pompidou research group (Université de Paris, Assistance Publique-Hôpitaux de Paris and Inserm UMR1153**)**: Sébastien Czernichow, Claire Carette, Charles Barsamian

Avicenne hospital group (Université Paris 13, Assistance publique-Hôpitaux de Paris and Inserm U955, Université Paris-Est, Créteil): Dominique Roulot-Marullo, Hélène Bihan, Emmanuel Cosson

Physics for Medicine Paris group (Inserm, CNRS and Ecole supérieur de Physique et Chimie de Paris ESPCI): Mickael Tanter, Thomas Deffieux, Sofiane Decombas, Thu-mai Nguyen

Biomedical imagery lab group (Inserm, Sorbonne Université and CNRS): Olivier Couture, Rachel Baida

Département d'Epidémiologie, Biostatistiques et Recherche Clinique HUPNVS (Université de Paris, Assistance Publique-Hôpitaux de Paris Inserm IAME-UMR1137 and URC PNVS): Cédric Laouénan, Jimmy Mullaert, Delphine Bachelet, Nathalie Gault, Estelle Marcault, Nassima Si-Mohammed, Pauline Manchon, Basma Basli-Baillet, Krishna Bhavsar

Unité de Recherche clinique en Economie de la Santé – Ile de France (URC-Eco) (Université Paris 12, Assistance Publique-Hôpitaux de Paris): Isabelle Durand Zaleski

Servier group: Nathalie de Préville, Philippe Delerive, Tania Baltauss, Erwan Werner, Laura Xuereb, Julia Geronimi, Jessica Laplume, Valérie Duvivier, Pierre Barbier Saint Hilaire, Edwige-Ludiwyne Balzac

Swiss Institute of Bioinformatics group: Mark Ibberson, Olivier Martin, Manuela Pruess

BioPrédictive: Thierry Poynard, Olivier Deckmyn

Commissariat à l'Energie Atomique: Christophe Junot, François Fenaille, Florence Castelli, Benoit Colsch

Supplementary material and methods

ATP content determination: PCLS viability was in part assessed *via* ATP content determination as described below [1]. Briefly, PCLS were homogenized in 500 µL of 2 mmol/L EDTA - 70% ethanol solution (pH 10.9) using a TissueLyser LT (Qiagen). ATP content was determined using the bioluminescent CellTiter-Glo® 3D Cell Viability Assay (Promega G9681) according to the manufacturer's instructions. Luminescence was recorded with a Fluoroskan FL microplate reader (ThermoFisher Scientific). ATP content was normalized to total protein content of the slice as measured by the Bradford Protein Assay (Bio-Rad). Presented results are expressed as the mean of the two slices for each condition.

RNA extraction and quantitative polymerase chain reaction: mRNA from PCLS were extracted in TRIzol® reagent (Life technologies) according to manufacturers' instructions. cDNA synthesis was performed with QuantiTect Reverse Transcription Kit (Qiagen). Quantitative polymerase chain reaction (qPCR) was performed on Real-Time PCR system LightCycler® 96 Instrument (Roche) using TaqMan® probes (Appliedbiosystems) with the following parameters: 1 cycle at 95°C for 10 min followed by 45 cycles at 95°C for 15s, 60°C for 60s. Probes references are detailed in Table S4. Gene expression was normalized to four housekeeping genes (*18s*, *GAPDH, HPRT1* and *PPIA*). Relative expression was calculated using the 2-delta-delta CT method and geometric average of normalization to each housekeeping gene was calculated. Presented results are expressed as the mean of the two slices for each condition.

Western blot: Snap frozen PCLS were homogenized in 200 µL RIPA buffer containing 150 mmol/L NaCl, 50 mmol/L TrisHCl, pH 7.4, 2 mmol/L EDTA, 0.5% sodium deoxycholate, 0.2% sodium dodecyl sulfate, 2 mmol/L activated orthovanadate, complete protease inhibitor cocktail tablet (cOmplete™, Roche) and complete phosphatase inhibitor cocktail tablet (PhosSTOP™, Roche). Homogenates were then incubated at 4°C for 45 minutes. Lysates were centrifuged at 12000 g for 5 min. Supernatants were collected and protein content was

quantified using the Lowry protein assay (Bio-Rad; Hercules, CA). Lysates were mixed with the reducing sample buffer for electrophoresis and subsequently transferred onto nitrocellulose membrane (Bio-Rad). Equal loading was checked using Ponceau red solution. Membranes were incubated with primary antibodies (primary antibodies used for western blot analyses are described in Table S5). After secondary antibody incubation (anti-rabbit or anti-mouse, Amersham, GE Healthcare, 1/3000), immunodetection was performed using an enhanced chemiluminescence kit (Immun-Star Western C kit, Bio-Rad). Bands were revealed using the ChemiDoc imaging system (Bio-Rad). Values reported from Western blots were obtained by band density analysis using Image Lab software (Bio-Rad) and expressed as the ratio of protein of interest on total loaded proteins (ponceau) for the whole cell extract.

Triglyceride and GSH contents determination: Snap frozen PCLS were homogenized in 500 μL PBS using a TissueLyser LT (Qiagen). Triglyceride content was determined using the bioluminescent Triglyceride-Glo™ Assay (Promega J3160) and GSH content was determined using the GSH-Glo™ Glutathione Assay (Promega V6911) according to the manufacturer's instructions. Luminescence was recorded with a Fluoroskan FL microplate reader (ThermoFisher Scientific). Triglyceride and GSH contents were normalized to total protein content of the slice as measured by the Bradford Protein Assay (Bio-Rad).

Histopathology and immunohistochemistry: PCLS were fixed in 10% formalin for 24 hours and embedded in paraffin with an automated carousel processor for dehydration, and paraffin embedding (Leica). Histopathology and immunostainings were performed using standard clinical procedures in the Pathology department of Beaujon Hospital (Clichy, France). Briefly, 3 μm thickness sections were made and stained with Hematoxylin and Eosin or Sirius red. Immunostainings for alpha-smooth muscle actin (α-SMA), CD68, phospho-Histone H2A.X (p-H2A.X) and cleaved Caspase-3 were performed with an automated immunohistochemical stainer (Ventana Benchmark®) according to the manufacturer's instructions (primary antibodies used for immunohistochemistry analyses are described in Table S5). Stained and immunostained slides were digitized (Scanscope AT turbo®, Leica). Steatosis was scored on

Hematoxylin and Eosin staining by a pathologist (VP) in a blinded manner, according to the following scoring system that assesses the proportion of large or medium fat droplets containing hepatocytes: S0: <5%; S1: 5–33%; S2: 34–66%; S3: >67% [2]. Quantitative analyses of immunostainings (α-SMA, cleaved Caspase-3 and CD68) and sirius red staining was performed using positive pixels algorithm (Indica Labs) on digital slides with Aperio software. Results are expressed as the percentage of positive pixels. p-H2A.X immunostaining analysis was performed using positive cells algorithm on digital slides with Qupath software and expressed as the percentage of positive nuclei. Quantification methods were automated observer-independent process based on whole-slide scanning.

Culture supernatants preparation and biochemical measurements: PCLS culture supernatants were collected after the 48th hour of culture and centrifuged for 15 minutes at 600g in order to remove cell debris. Supernatants were aliquoted and stored at -80°C until use. Aspartate aminotransferase (AST) level were measured by colorimetric assay (Cohesion Biosources CAK1004) according to the manufacturer's instructions. Absorbance at 520 nm was recorded with a Multiskan sky microplate reader (ThermoFisher Scientific). LDH and glucose levels were measured in PCLS supernatants by standard clinical procedures at Beaujon Hospital (Clichy, France).

Transcriptomic analysis: mRNA from PCLS were extracted in TRIzol® reagent reagent (Life technologies) according to manufacturer's instructions. To monitor modulated genes following Elafibranor or S217879 treatments, an RNA library was prepared using the SMARTer® Stranded Total RNA-Seq Kit v3 (Pico Input Mammalian) according to manufacturer's recommendations (634873, Takara). Samples were sequenced on ILLUMINA Novaseq 6000 with S1-200 cartridge in the iGenSeq core facility (Genotyping and sequencing), at Institut du Cerveau (Paris, France). Raw RNA-seq reads were mapped to the human genome (Ensembl GRCH38) and Ensembl's reference transcriptome using STAR [3]. Gene counts were obtained using FeatureCount [4], normalized by an UpperQuartile procedure, and logged on a base 2. RNAseq analyses were performed by JR Analytics (jr-analytics.fr). Genes from sexual

chromosomes and genes with null variance were removed prior normalization. Raw Gene expression profiles were normalized using the upper-quartile approach and log2+1 transformed [5]. Analyses were corrected for gender effects. Differential gene expression between groups (Elafibranor *vs.* DMSO, and S217879 *vs.* DMSO, and Elafibranor *vs.* S217879) were estimated and the statistical relevance evaluated with Student's t test. Gene set enrichment analysis (GSEA) was performed using the fast GSEA implementation (10.18129/B9.bioc.fgsea; Bioconductor, open-source software), preranked by the t.test value from the studied comparison. Leading edges of gene set enrichment (genes having the most impact in the enrichment pathway) were displayed as a heatmaps.

RNA sequencing data presented here have been deposited in NCBI's Gene Expression Omnibus and are accessible through GEO Series accession number GSE234415 (https://www.ncbi.nlm.nih.gov/geo/query/acc.cgi?acc=GSE234415).

Supplementary figures

Figure S1

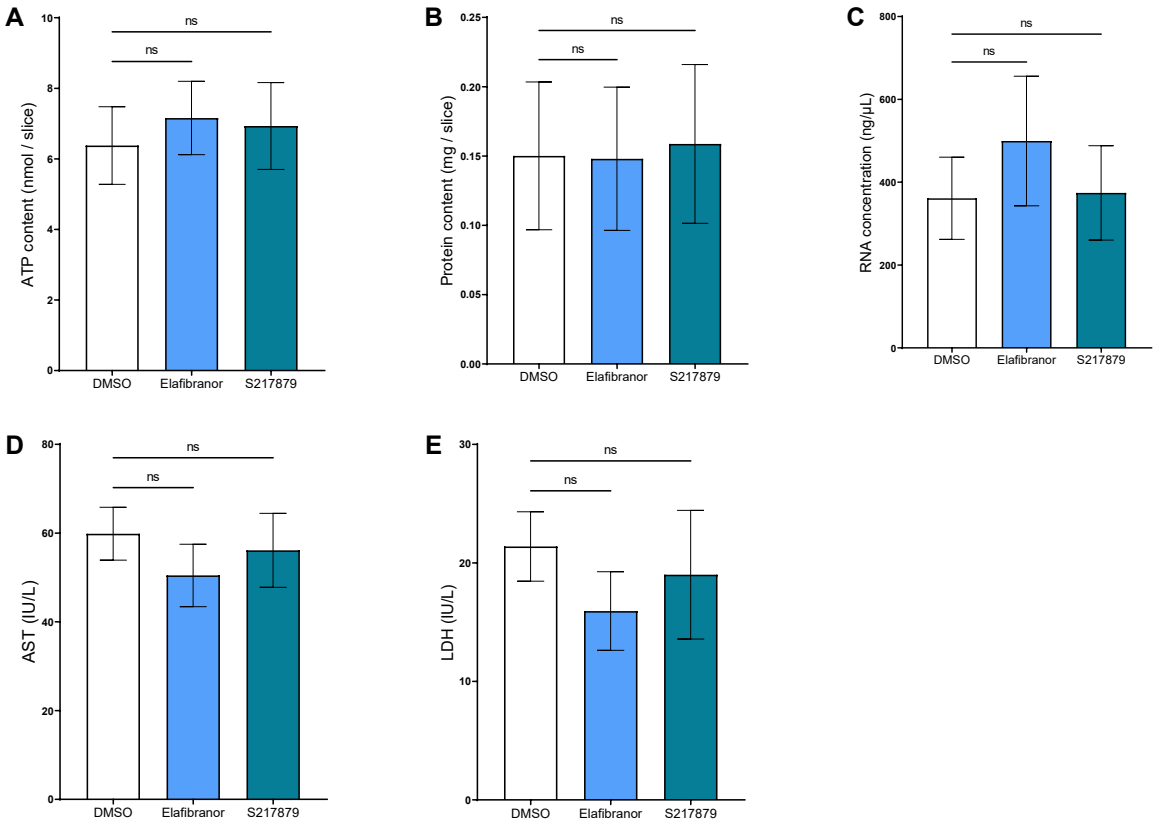

Fig. S1: Drugs safety. Human PCLS were generated from the liver of patients with MAFLD and treated with Elafibranor (10 µM) or S217879 (3 µM) or vehicle (DMSO, 0.1%) for two days. (**A**) Quantification of ATP, (**B**) protein and (**C**) RNA contents in human PCLS with MAFLD. (**D**) Quantification of AST and (**D**) LDH levels in PCLS culture supernatants. n=12 PCLS per condition generated from 12 patients with MAFLD. Data are expressed as mean ± SEM. ns, not significant (Wilcoxon paired t-test). MAFLD, metabolic associated fatty liver disease; PCLS, precision cut liver slices.

Figure S2

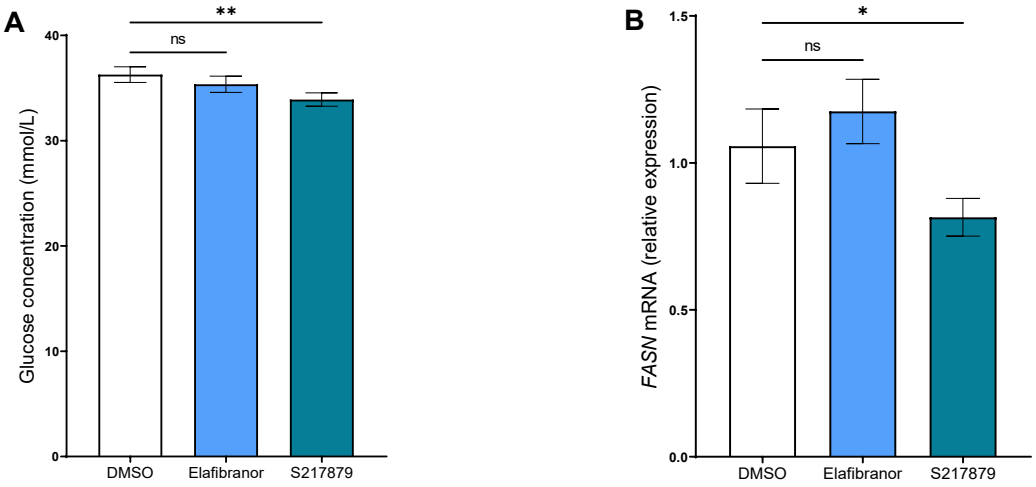

Fig. S2: S217879 but not Elafibranor inhibits neoglucogenesis and *de novo* lipogenesis. Human PCLS were generated from the liver of patients with MAFLD and treated with Elafibranor (10 µM) or S217879 (3 µM) or vehicle (DMSO, 0.1%) for two days. (**A**) Quantification of glucose concentration in PCLS culture supernatants. (**B**) qPCR analysis of *FASN* expression in human PCLS with MAFLD. n=12 PCLS per condition generated from 12 patients with MAFLD. Data are expressed as mean ± SEM. *p<0.05; **p<0.01; ns, not significant (Wilcoxon paired t-test). MAFLD, metabolic associated fatty liver disease; PCLS, precision cut liver slices.

Figure S3

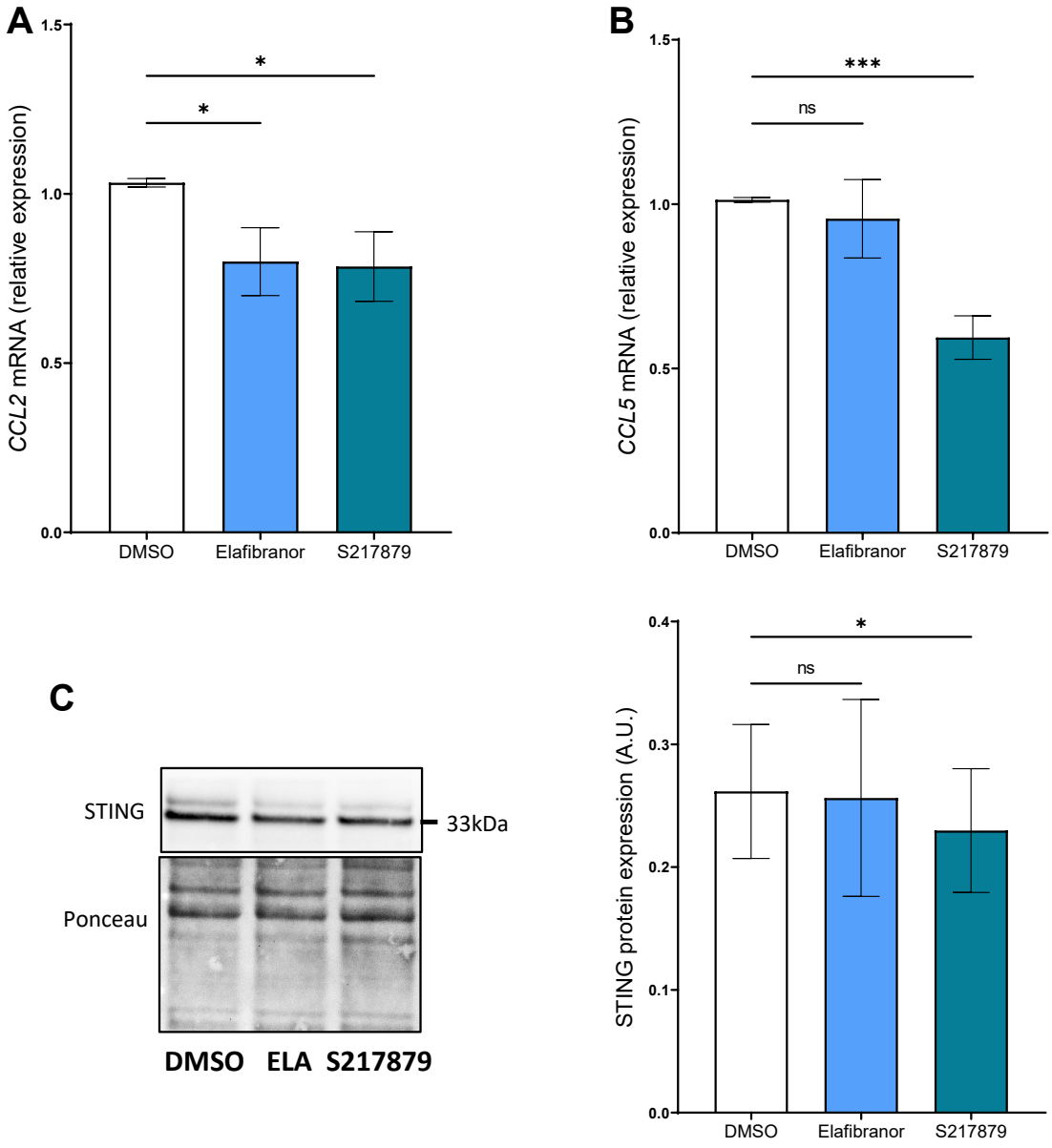

Fig. S3: Elafibranor and S217879 reduce liver inflammation. Human PCLS were generated from the liver of patients with MAFLD and treated with Elafibranor (10 µM) or S217879 (3 µM) or vehicle (DMSO, 0.1%) for two days. (**A**) qPCR analysis of *CCL2* and (**B**) *CCL5* expression in human PCLS with MAFLD. (**C**) Immunoblot analysis of STING expression in human PCLS with MAFLD. n=12 PCLS per condition generated from 12 patients with MAFLD. Data are expressed as mean ± SEM. *p<0.05; ***p<0.001; ns, not significant (Wilcoxon paired t-test). MAFLD, metabolic associated fatty liver disease; PCLS, precision cut liver slices.

Figure S4

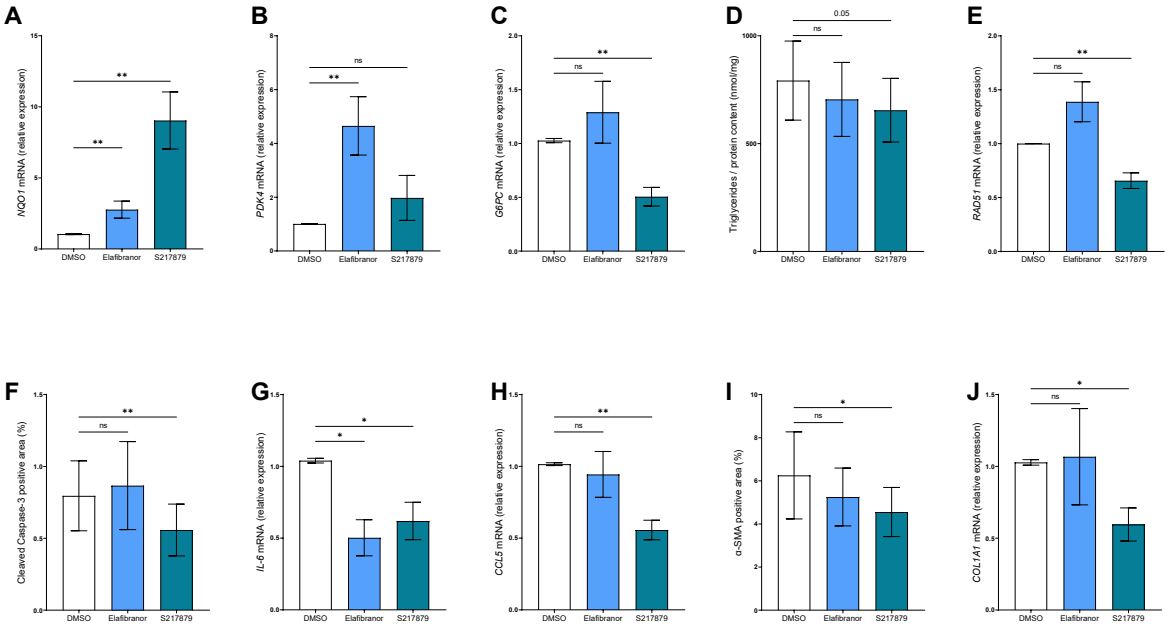

Fig. S4: Effects of Elafibranor and S217879 on PCLS from patients with advanced liver fibrosis. Human PCLS were generated from the liver of patients with MAFLD with advanced liver fibrosis (F3-F4, n=9 patients) and treated with Elafibranor (10 µM) or S217879 (3 µM) or vehicle (DMSO, 0.1%) for two days. qPCR analysis of *NQO1* (**A**), *PDK4* (**B**), and *G6PC* (**C**) expression in PCLS with MAFLD from patients with advanced liver fibrosis. (**D**) Quantification of triglycerides content (Triglycerides/protein content ratio) in PCLS with MAFLD from patients with advanced liver fibrosis. (**E**) qPCR analysis of *RAD51* expression in PCLS with MAFLD from patients with advanced liver fibrosis. (**F**) Immunohistochemical analysis of cleaved Caspase-3 positive area (%) on PCLS with MAFLD from patients with advanced liver fibrosis. (**G**) qPCR analysis of *IL-6* and (**H**) *CCL5* expression in PCLS with MAFLD from patients with advanced liver fibrosis. (**I**) Immunohistochemical analysis of α-SMA positive area (%) on PCLS with MAFLD from patients with advanced liver fibrosis. (**G**) qPCR analysis of *COL1A1* expression in PCLS with MAFLD from patients with advanced liver fibrosis. Data are expressed as mean ± SEM. *p<0.05; **p<0.01; ns, not significant (Wilcoxon paired t-test). Same patients were used in the analyses of drugs effects in patients with all stages of fibrosis (Figures 1-5, 7). MAFLD, metabolic associated fatty liver disease; PCLS, precision cut liver slices.

Figure S5

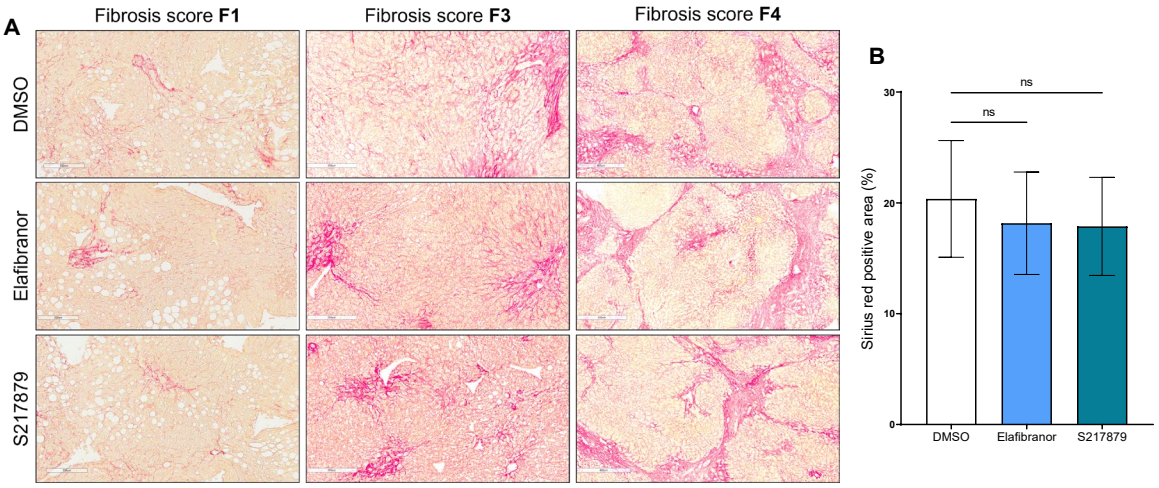

Fig. S5: Elafibranor and S217879 does not affect liver fibrosis. Human PCLS were generated from the liver of patients with MAFLD and treated with Elafibranor (10 µM) or S217879 (3 µM) or vehicle (DMSO, 0.1%) for two days. Fibrosis deposition was evaluated on Sirius red staining. (**A**) Representative images of histological analysis of liver fibrosis on Sirius red staining on PCLS sections from patients with F1, F3 or F4 fibrosis score [2]. (**B**) Quantification of liver fibrosis area on Sirius red stained slides. n=12 PCLS per condition generated from 12 patients with MAFLD. Data are expressed as mean ± SEM. ns, not significant (Wilcoxon paired t-test). MAFLD, metabolic associated fatty liver disease; PCLS, precision cut liver slices.

Figure S6

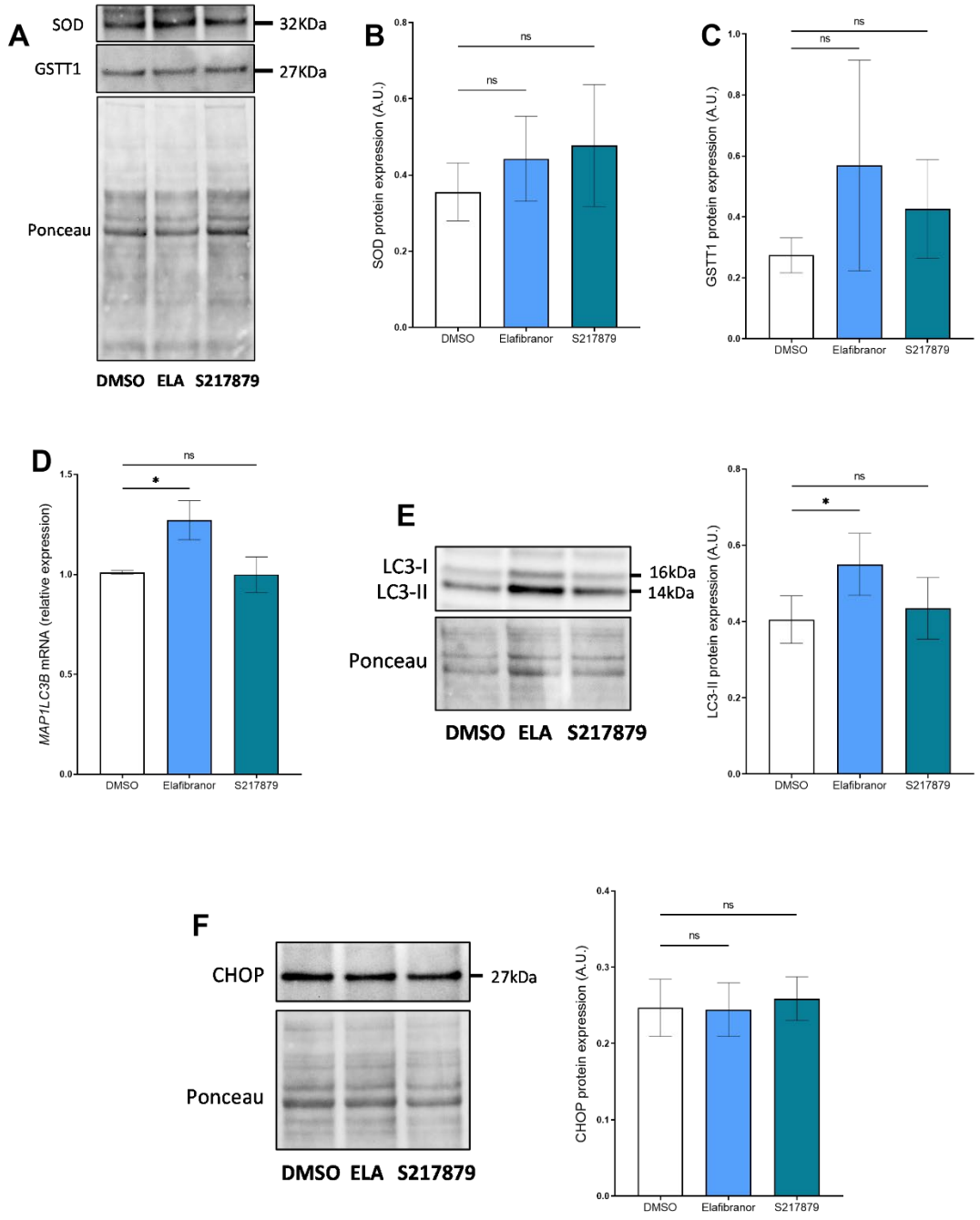

Fig. S6: Effects of Elafibranor and S217879 on liver autophagy and ER-stress. Human PCLS were generated from the liver of patients with MAFLD and treated with Elafibranor (10 µM) or S217879 (3 µM) or vehicle (DMSO, 0.1%) for two days. (**A**) Representative western blotting of SOD and GSTT1 expression. (**B**) Quantification of SOD and (**C**) GSTT1 protein expression. (**D**) qPCR analysis of LC3 expression (*MAP1LC3B*) in human PCLS with MAFLD. (**E**) Immunoblot analysis of LC3-II expression in human PCLS with MAFLD. (**F**) Immunoblot

analysis of CHOP expression in human PCLS with MAFLD. Data are expressed as mean ± SEM. n=12 PCLS per condition generated from 12 patients with MAFLD. *p<0.05; ns, not significant (Wilcoxon paired t-test). GSTT1, Glutathione S-Transferase Theta 1; MAFLD, metabolic associated fatty liver disease; PCLS, precision cut liver slices; SOD, superoxide dismutase.

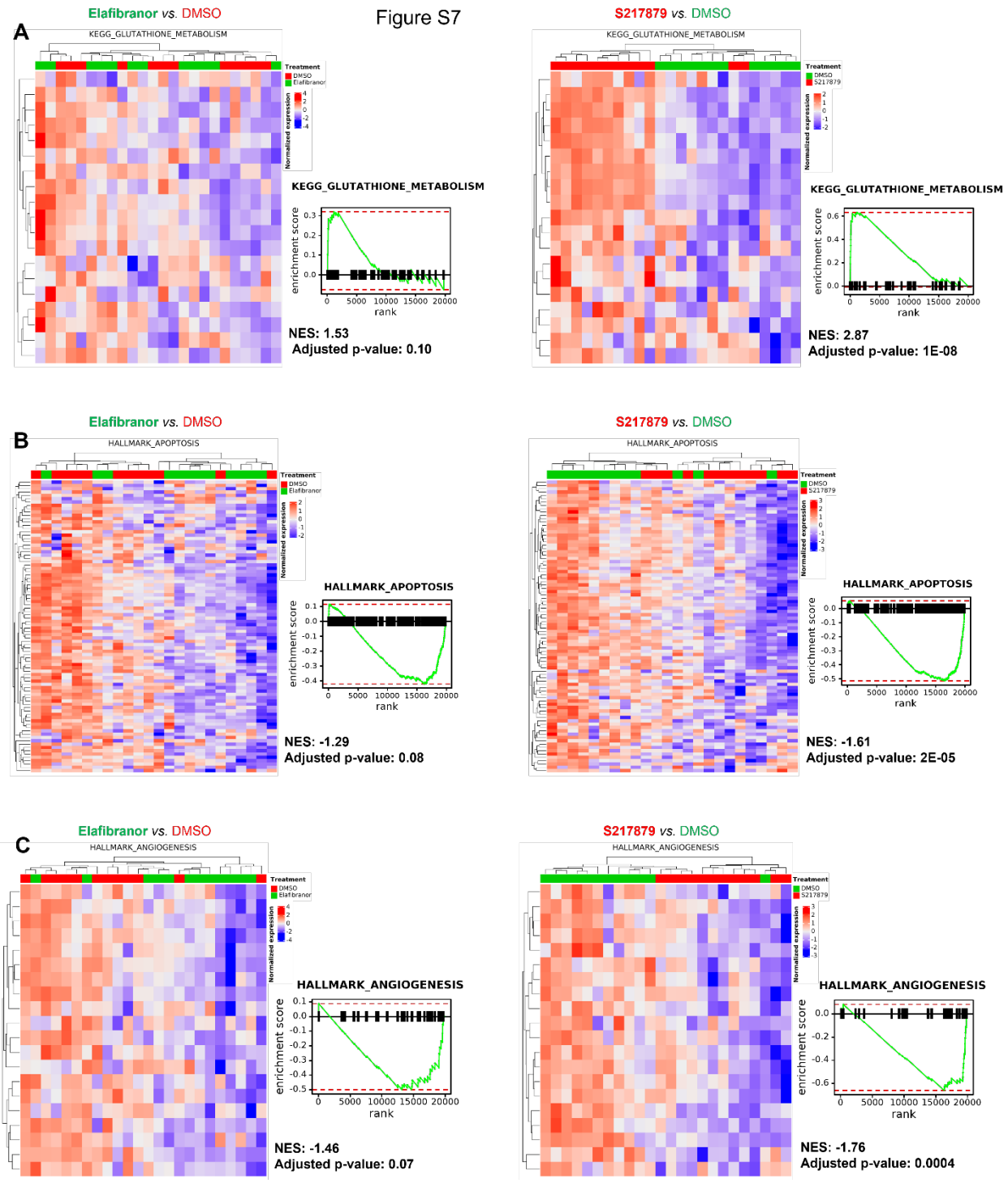

Fig. S7: S217879 treatment induces a potent anti-oxidant response and inhibits apoptosis and angiogenesis. Human PCLS were generated from the liver of patients with MAFLD and treated with Elafibranor (10 µM) or S217879 (3 µM) or vehicle (DMSO, 0.1%) for two days. (**A**) Heatmaps and enrichment plots of differentially expressed genes in glutathione metabolism, (**B**) apoptosis, and (**C**) angiogenesis pathways in Elafibranor and S217879-

treated PCLS *vs.* vehicle treated-PCLS. n=12 PCLS per condition generated from 12 patients with MAFLD. MAFLD, metabolic associated fatty liver disease; NES, normalized enrichment score; PCLS, precision cut liver slices.

Figure S8

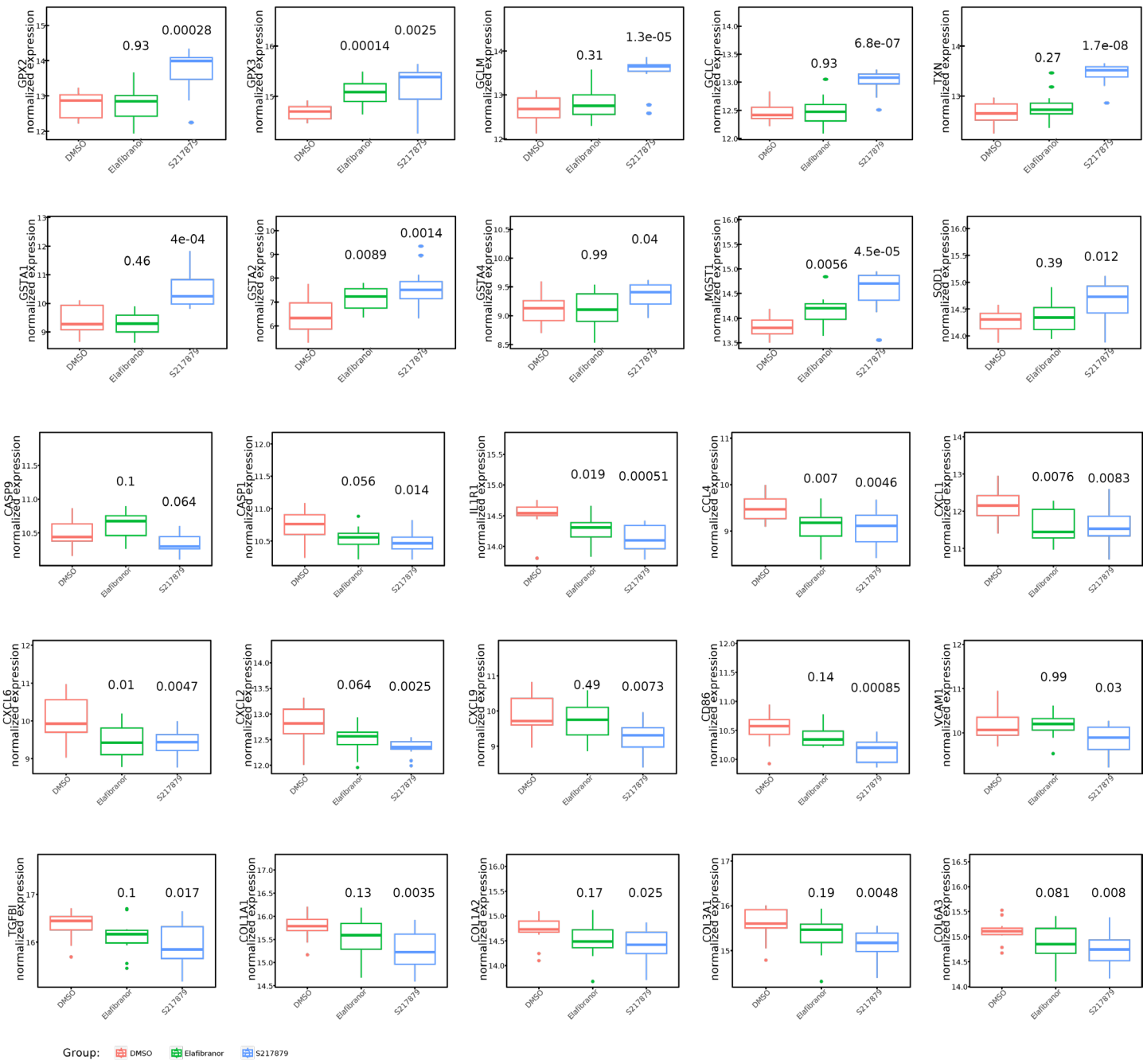

Fig. S8: Differentially expressed genes in Elafibranor and S217879-treated PCLS *vs.* vehicle-treated PCLS. Human PCLS were generated from the liver of patients with MAFLD and treated with Elafibranor (10 µM) or S217879 (3 µM) or vehicle (DMSO, 0.1%) for two days (n=12 PCLS per condition from 12 patients with MAFLD). Gene expression was evaluated on RNA sequencing data and are expressed as normalized counts.

Figure S9

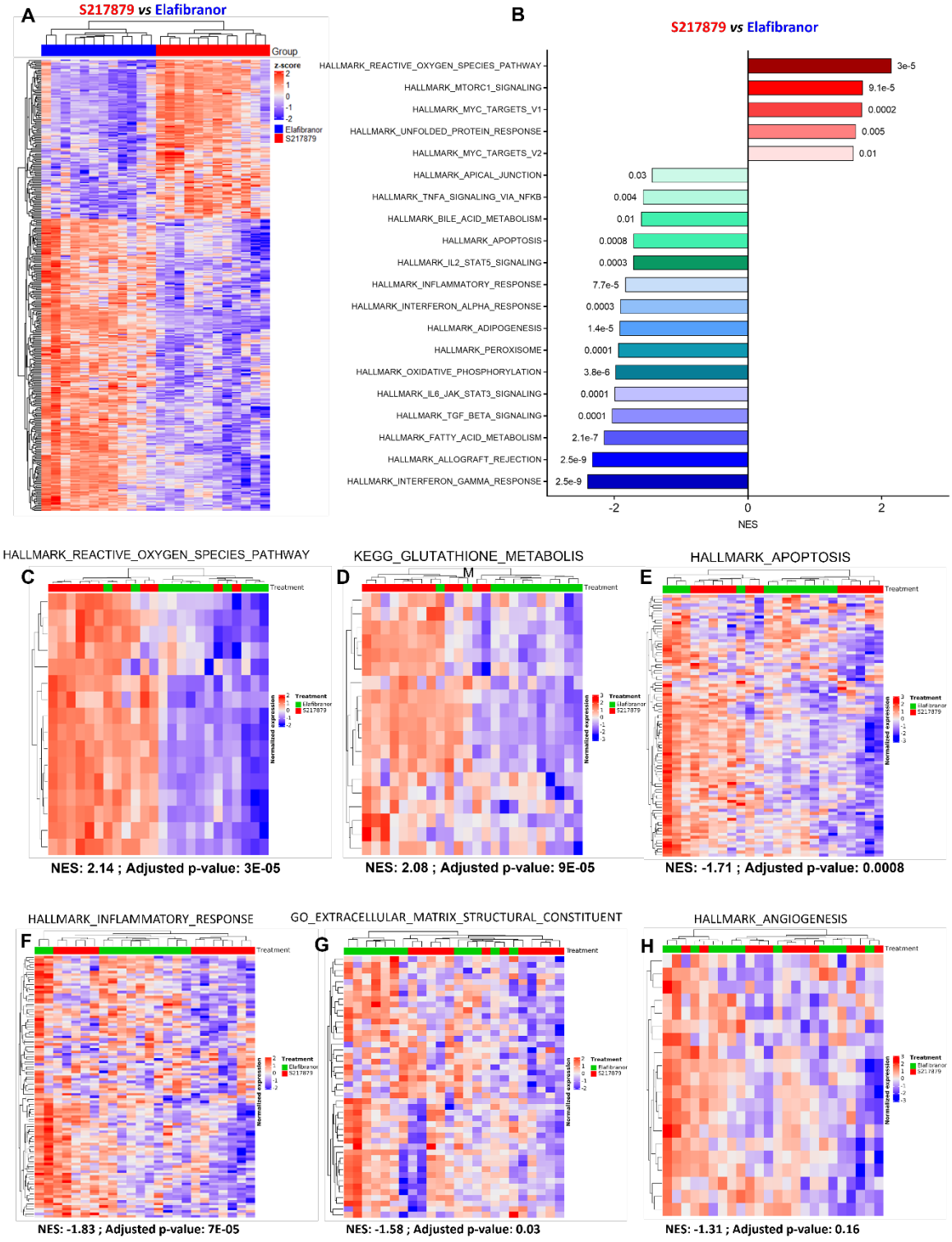

Fig. S9: S217879 has more pronounced effects than Elafibranor to inhibit pathways involved in NASH. Human PCLS were generated from the liver of patients with MAFLD and treated with Elafibranor (10 µM) or S217879 (3 µM) or vehicle (DMSO, 0.1%) for two days. (**A**) Heatmap of significantly differentially expressed genes from S217879 *vs.* Elafibranor-treated

PCLS (FDR-adjusted p-value cut-off: 0.05). (**B**) Gene set-enrichment analysis of most differentially modulated pathways in S217879 *vs.* Elafibranor-treated PCLS with MAFLD. (**C**) Heatmaps of differentially expressed genes in reactive oxygen species, (**D**) glutathione metabolism, (**E**) apoptosis, (**F**) inflammatory response, (**G**) extracellular matrix structural constituent, and (**H**) angiogenesis pathways in S217879 *vs.* Elafibranor-treated PCLS with MAFLD. n=12 PCLS per condition generated from 12 patients with MAFLD. MAFLD, metabolic associated fatty liver disease; NES, normalized enrichment score; PCLS, precision cut liver slices.

Supplementary tables

Supplementary Table S1. Patients' characteristics

					Non tumoral liver used for PCLS	
Patient n°	**Gender**	**Age**	**Indication for surgery**	**Alcohol consumption**	**SAF** [2]	**NAS** [6]
1	F	67	Liver metastases from colon adenocarcinoma	No	S2A1F1	2+0+1=3
2	F	65	Cholangiocarcinoma	No	S1A3F4	1+1+2=4
3	M	65	Hepatocellular carcinoma	Yes	S1A1F3	1+0+1=2
4	F	66	Hepatocellular carcinoma	No	S0A4F4	0+3+2=5
5	M	51	Hepatocellular carcinoma	Yes	S2A3F3	2+1+1=4
6	M	52	Focal nodular hyperplasia	Yes	S1A1F3	1+1+0=2
7	F	67	Non-transplantable liver	No	S1A0F1	1+0+0=1
8	F	48	Neuroendocrine tumor	No	S1A0F1	1+0+0=1
9	M	58	Hepatocellular carcinoma	Yes	S2A3F3	2+1+1=4
10	M	74	Hepatocellular carcinoma	No	S0A3F4	0+1+1=2
11	F	74	Hepatocellular carcinoma	No	S1A4F3	1+2+2=5
12	F	68	Hepatocellular carcinoma	Yes	S1A3F4	1+1+2=4

Abbreviations: NAS, NAFLD activity score; SAF, steatosis, activity, fibrosis score; PCLS, precision cut liver slices.

Supplementary Table S2. Patients' metabolic and morphological features

Metabolic and morphological features	
Age (years)	65.5 (53.5 - 67.7)
Female gender (n, %)	7 (58.3 %)
BMI (Kg/m²)	30.4 (29.3 - 34.7)
Type 2 diabetes (n, %)	6 (50 %)
Fasting serum glucose (g/L)	1.53 (1.20 - 2.40)
Serum AST (IU/L)	46.0 (32.0 - 57.0)
Serum ALT (IU/L)	47.0 (24.0 - 68.0)
Serum gamma-GT (IU/L)	108.0 (37.0 - 125.0)

Abbreviations: ALT, alanine aminotransferase; AST, aspartate aminotransferase; BMI, body mass index; gamma-GT, gamma-glutamyl transpeptidase. n=12 patients. Data are expressed as median ± IQR or n (%) for the gender and type 2 diabetes.

Supplementary Table S3. Characteristics of patients used for autophagic flux evaluation after Elafibranor or S217879 treatment with choloroquine

				Non tumoral liver used for PCLS	
Patient n°	**Gender**	**Age**	**Indication for surgery**	**SAF**	**NAS**
1	F	67	Rejected liver graft	S1A0F1	1+0+0=1
2	F	42	Liver metastases from colon cancer	S1A0F0	1+0+0=1
3	M	65	Vesicular adenocarcinoma	S0A0F0	0+0+0=0
4	F	48	Neuroendocrine tumor	S1A0F1	1+0+0=1
5	M	84	Hepatocellular carcinoma	S0A0F0	0+0+0=0
6	M	58	Hepatocellular carcinoma	S2A3F3	2+1+1=4
7	M	74	Hepatocellular carcinoma	S0A3F4	0+1+1=2
8	F	74	Hepatocellular carcinoma	S1A4F3	1+2+2=5
9	M	68	Hepatocellular carcinoma	S0A0F4	0+0+0=0
10	F	68	NASH related cirrhosis	S1A3F4	1+1+2=4
11	M	69	Hepatocellular carcinoma	S1A1F3	1+0+1=2

Abbreviations: NAS, NAFLD activity score; SAF, steatosis, activity, fibrosis score. PCLS, precision cut liver slices.

Supplementary Table S4. Taqman probes used for qPCR analyses

Gene	Life technologies Taqman probe ID
18S	Hs03003631_g1
ACOX1	Hs01074241_m1
ACTA2	Hs00426835_g1
CCL2	Hs00234140_m1
CCL5	Hs00982282_m1
COL1A1	Hs00164004_m1
COL1A2	Hs01028956_m1
CPT1A	Hs00912671_m1
FASN	Hs01005622_m1
FGF21	Hs00173927_m1
G6PC	Hs02802676_m1
GAPDH	Hs02786624_g1
GPX2	Hs01591589_m1
GPX3	Hs01078668_m1
GSTA2	Hs00747232_mH
HMOX1	Hs01110250_m1
HPRT1	Hs02800695_m1
IL-1β	Hs01555410_m1
IL-6	Hs00174131_m1
MAP1LC3B	Hs00797944_s1
NQO1	Hs02512143_s1
PDK4	Hs01037712_m1
PPARA	Hs00947536_m1
PPIA	Hs04194521_s1
RAD51	Hs00947967_m1
SREBF1	Hs01088679_g1
XRCC1	Hs00959834_m1

Supplementary Table S5. List of antibodies used for western blots and immunostaining analyses

Antibody anti-	Raised in	Reference	Dilution	WB buffer	IHC buffer
α-SMA	Mouse	Sigma Aldrich A2547	1/1000	TBST milk	-
α-SMA	Mouse	Dako M0851	1/600	-	PBS BSA
Cleaved Caspase-3	Rabbit	CST 9661	1/400	-	PBS BSA
CD68	Mouse	Dako M0814	1/500	-	PBS BSA
CHOP	Mouse	CST 2895	1/1000	TBST milk	-
MGST1	Rabbit	Abcam ab131059	1/1000	TBST milk	-
GPX2	Rabbit	Abcam ab137431	1/1000	TBST milk	-
GSTM2	Rabbit	ABclonal A13496	1/1000	TBST milk	-
GSTT1	Rabbit	Abcam ab199337	1/1000	TBST milk	-
ICAM-1	Rabbit	CST 67836	1/1000	TBST milk	-
LC3-B	Rabbit	CST 2775	1/1000	TBST milk	-
p-H2A.X	Rabbit	CST 9718	1/20000	TBST milk	-
p-H2A.X	Rabbit	Abcam ab81299	1/200	-	PBS BSA
SOD	Rabbit	Abcam ab179843	1/1000	TBST milk	-
STING	Rabbit	CST 13647	1/1000	TBST milk	-
VCAM-1	Rabbit	CST 13662	1/1000	TBST milk	-

Abbreviations: BSA, bovine serum albumin; CST, cell signaling technology; IHC, immunohistochemistry; LC3, light chain 3; PBS, phosphate buffer saline; TBST, tris buffer saline 0.05 tween; WB, western blot.

References

[1] de Graaf IAM, Olinga P, de Jager MH, Merema MT, de Kanter R, van de Kerkhof EG, et al. Preparation and incubation of precision-cut liver and intestinal slices for application in drug metabolism and toxicity studies. Nat Protoc 2010;5:1540–51. https://doi.org/10.1038/nprot.2010.111.

[2] Bedossa P, Poitou C, Veyrie N, Bouillot J-L, Basdevant A, Paradis V, et al. Histopathological algorithm and scoring system for evaluation of liver lesions in morbidly obese patients. Hepatol Baltim Md 2012;56:1751–9. https://doi.org/10.1002/hep.25889.

[3] Dobin A, Davis CA, Schlesinger F, Drenkow J, Zaleski C, Jha S, et al. STAR: ultrafast universal RNA-seq aligner. Bioinforma Oxf Engl 2013;29:15–21. https://doi.org/10.1093/bioinformatics/bts635.

[4] Liao Y, Smyth GK, Shi W. featureCounts: an efficient general purpose program for assigning sequence reads to genomic features. Bioinforma Oxf Engl 2014;30:923–30. https://doi.org/10.1093/bioinformatics/btt656.

[5] Bullard JH, Purdom E, Hansen KD, Dudoit S. Evaluation of statistical methods for normalization and differential expression in mRNA-Seq experiments. BMC Bioinformatics 2010;11:94. https://doi.org/10.1186/1471-2105-11-94.

[6] Kleiner DE, Brunt EM, Van Natta M, Behling C, Contos MJ, Cummings OW, et al. Design and validation of a histological scoring system for nonalcoholic fatty liver disease. Hepatol Baltim Md 2005;41:1313–21. https://doi.org/10.1002/hep.20701.